

Article

An Analysis on the Effectiveness of Nitrogen Oxide Reduction from Applying Titanium Dioxide on Urban Roads Using a Statistical Method

Sang-Hyuk Lee, Jong-Won Lee, Moon-Kyung Kim and Hee-Mun Park *

Korea Institute of Civil Engineering and Building Technology, Gyeonggi-do 10223, Korea; slee@kict.re.kr (S.-H.L.); asca28@kict.re.kr (J.-W.L.); moonkyung@kict.re.kr (M.-K.K.)

* Correspondence: hpark@kict.re.kr; Tel.: +82-91-910-0323

Abstract: The purpose of this study was to analyze the effect of titanium dioxide (TiO₂) on reducing nitrogen oxide (NO_x) concentrations using the statistical method of the Anderson-Darling test. To compare and analyze this effect, a spray-type form of TiO₂ was applied to the asphalt pavement surface on urban roads. Data acquisition for NO_x concentration was collected from a test section with TiO₂ applied and a reference section without TiO₂ applied. The probabilities of occurrence of the NO_x concentration in the test and reference section were estimated and compared using the Anderson-Darling test. In sum, most of the NO_x concentrations were probabilistically lower in the test section. The average probability of the NO_x concentration in the test section in the ‘low’ range was 46.2% higher than in the reference section. In the ‘high’ and ‘moderate’ ranges, the average probability of the NO_x concentration compared to that of the reference section was lower by 28.1% and 18.8%, respectively. These results revealed that the photochemical reaction from the TiO₂ material applied on asphalt pavement was effective in reducing NO_x.



Citation: Lee, S.-H.; Lee, J.-W.; Kim, M.-K.; Park, H.-M. An Analysis on the Effectiveness of Nitrogen Oxide Reduction from Applying Titanium Dioxide on Urban Roads Using a Statistical Method. *Atmosphere* **2021**, *12*, 972. <https://doi.org/10.3390/atmos12080972>

Academic Editor: Lise Lotte Sørensen

Received: 22 June 2021

Accepted: 26 July 2021

Published: 28 July 2021

Publisher's Note: MDPI stays neutral with regard to jurisdictional claims in published maps and institutional affiliations.



Copyright: © 2021 by the authors. Licensee MDPI, Basel, Switzerland. This article is an open access article distributed under the terms and conditions of the Creative Commons Attribution (CC BY) license (<https://creativecommons.org/licenses/by/4.0/>).

Keywords: titanium dioxide; nitrogen oxide concentration; Anderson-Darling test; photocatalyst

1. Introduction

The steady growth in economic conditions and the rapid increase in the economic growth of neighboring countries in the past several decades have led to an accelerated degree of air pollution in South Korea. Most notably among air pollution issues is the widely discussed social issue regarding the increase of particulate matter concentrations to a serious level due to migration from neighboring countries and seasonal effects.

Particulate matter is defined by the US EPA as a complex of extremely small particles and liquid droplets. Particulate matter can be generally classified into two categories: particulate matter with less than 10 µm in diameter (PM₁₀) and particulate matter with less than 2.5 µm in diameter (PM_{2.5}), which are called fine particulate matter. Sources of particulate matter are known to include the combustion process at manufacturing industries, especially industrial plants that contribute more than 60%, while roads and non-point pollution sources, energy industry combustion and other production processes are known to each take up about 20%, respectively. Also, air pollutants emitted into the atmosphere can be the source of secondary pollutants that are further converted into particulate matter through chemical reactions [1]. PM_{2.5} consists of pollutants containing heavy metals, sulfur dioxide (SO₂), nitrogen oxide (NO_x), lead (Pb), ozone (O₃), and carbon monoxide (CO). They can be generally produced through chemical reactions that combine SO₂ and NO_x from fossil fuel combustion and vehicle emissions with water vapor and ozone. NO_x compounds can negatively affect human health, and the nitric acid and nitrate formed by the oxidation of NO_x are the main sources of nitric acid rain that can have a negative effect on ecological environments [2]. Since NO_x is a main source of generating PM_{2.5} on urban roads, the technology development for reducing NO_x concentration is crucial.

Recently, a method using titanium dioxide (TiO_2) has been proposed to reduce NO_x concentration from air pollutions, and a number of studies have been carried out to remove NO_x by applying TiO_2 on urban road structures and highway areas [3]. However, few studies analyzing the NO_x reduction effect from applying TiO_2 on operating roads or highways have been carried out. Also, previously conducted studies had limitations in analyzing the reduction amount by measuring the NO_x concentration at a certain point of time after applying TiO_2 to the roads. Therefore, an analytical method is needed to better understand the NO_x reduction effect of TiO_2 material.

The objective of this study is to evaluate NO_x reduction efficiency using field measurement data and statistical analysis after applying TiO_2 on the pavement surface of urban roads. A liquid type of TiO_2 material was applied on the asphalt pavement surface at the test section. The reference section is defined as a section without TiO_2 applied for relative comparison analysis of NO_x reduction effect. NO_x concentration data was monitored in the test and reference sections simultaneously for ten days. In order to analyze the NO_x reduction effect of TiO_2 on urban roads, probability distributions for NO_x concentration were estimated using the statistical method of the Anderson-Darling test. Anderson-Darling test is a statistical goodness-of-fit verification method presented as a criterion for reducing errors in the process of estimation. This Anderson-Darling test is a useful method for accurate prediction and estimation of the NO_x reduction effect of TiO_2 through stochastic analysis. Therefore this method proposed in this study can carry out more accurate quantitative and qualitative analysis compared to existing methods. In addition, the occurrence probability of NO_x concentration was calculated using the probability density function for the estimated probability distribution to analyze the NO_x reduction effect in the test section.

2. Related Works

Since the late 20th century, many studies related to the occurrence of NO_x , particulate matter, and other air pollutants on urban roads have been actively conducted. In the 1970s, lots of studies focused on the direct effects of traffic characteristics on the occurrence of NO_x , SO_2 , CO , and O_3 [4,5]. In the 1990s, several studies were performed on the short-term effects of harmful emissions. According to the research of Katsouyanni et al., an increase of 50 mg/m^3 in SO_2 level was associated with a 3% increase in mortality, and a 2% increase in PM_{10} concentration [6].

In the early 2000s, some studies were carried out to investigate the long-term effects of harmful emissions. At the time, the World Health Organization (WHO) announced that NO_x from main roads is a major source of air pollution (40–50%). In addition, there are 30% more NO_x generated at road facilities such as tunnels, bridges, and highways compared to general roads [7]. Also, the European Environmental Agency published that exposure to NO_x was responsible for around 70,000 deaths in the European Union and approximately 400,000 premature deaths were caused by exposure to high particulate matter concentration levels [8]. As such, particulate matter formed by NO_x compounds from roads has a fatal effect on human health.

As part of a study on the perception and awareness of particulate matter pollution caused by urbanization and industrialization, Srimuruganandam and Nagendra sampled the 24-h average ambient particulate matter (PM_{10} and $\text{PM}_{2.5}$) concentration at two intersections in Chennai, India, from November 2008 to April 2009 [9]. The study results show that the 24-h average ambient particulate matter concentration was significantly higher in the winter and monsoon season than in the summer. The results also indicated that secondary particulate matter from traffic conditions (22.9% in PM_{10} , 42.1% in $\text{PM}_{2.5}$) was the major cause of higher particulate matter concentrations in the study area.

Jandacka and Durcanska measured particulate matter fraction concentrations (PM_{10} , $\text{PM}_{2.5}$, $\text{PM}_{1.0}$), substance concentration, and crystals at 6 different monitoring stations in Zilina, Slovakia, from 2017 to 2019 to find sources of particulate matter in urban areas [10]. The study results revealed that characteristics of particulate matter is dependent on mea-

suring stations and seasons. In particular, higher concentrations of particulate matter were measured due to differences in the concentration of chemical elements contained in particulate matter on the roads. This variation of particulate matter concentrations was caused not only by traffic volumes but also by weather conditions.

Photocatalytic oxidation is a useful and effective method to remove NO_x precursors. Therefore, many studies have been conducted recently with a focus on reduction of NO_x concentrations using photocatalytic oxidation [11–14].

Folli et al. examined the reduction of NO_x concentration after applying 100 mm thick double-cast concrete blocks containing TiO₂ in Copenhagen, Denmark [15]. This study presented that the average daily NO concentration in concrete blocks with TiO₂ was below 40 ppbv. Also, the NO reduction efficiency was higher in the summer than in the winter, and monthly average NO concentration in the photocatalytic section was about 22% lower than reference section during the summer. In particular, data measured around noon in the summer indicated that the average NO reduction efficiency is higher than 30% due to higher solar radiation.

Bocci et al. applied an asphalt emulsion and cement mortar with TiO₂ on the main and emergency lane of highway sections in Italy to analyze the applicability of photocatalyst material [16]. The effectiveness of photocatalytic treatments was evaluated by measuring NO reductions after 1, 17, 46, 88, 218, and 527 days from applying the proposed materials. The results show that all the products were effective after 24 h from the application with a 40% reduction efficiency for asphalt emulsion-based TiO₂ products and 23% reduction efficiency for cement mortar-based TiO₂ products. However, the reduction efficiency started to decrease gradually with elapsed time and the NO reduction efficiencies for asphalt and concretes products were 1.77% and 0.49% after 527 days, respectively. Moreover, the NO reduction efficiency of the main lane at a highway section was lower compared to the emergency lane at a highway section due to heavy vehicle traffic. The study also found that cement mortar-based TiO₂ products had faster performance degradation compared to asphalt emulsion-based TiO₂ products.

Wang et al. developed a new method for constructing photocatalytic air-purifying asphalt pavements and evaluated the feasibility and performance of new method [17]. This study adopted two ways to produce the TiO₂ modified aggregate, which were aggregate surface coating and pore filling. They investigated and compared the durability in terms of photocatalytic efficiency and mechanical performance under vehicle tire polishing. Both aggregate surface coating and pore filling methods produced satisfactory NO reduction rates around 40% before vehicle tire polishing but reduction efficiency was reduced in both methods after vehicle tire polishing. Comparing these two methods for NO reduction efficiency revealed that the pore filling method provided a better long-term NO reduction efficiency than aggregate surface coating method.

Yu et al. evaluated the NO_x degradation performance of nano-TiO₂ as a coating material for the road environment using the photocatalytic test system designed by this study under various radiation intensities [18]. The material used in this study were anatase nano-TiO₂, activated carbon powder, silane coupling agent and deionized water. Using the presented materials, the impact of varying amounts of coating material and silane coupling agent were evaluated. The results show that the material has acceptable photocatalytic degradation performance and the proper amount of silane coupling agent could enhance the bonding performance of the material and asphalt mixture. For the roadside coating, sodium dodecylbenzene sulfonate was selected as the surfactant to carry out the photocatalytic degradation experiment of NO₂ with different dosages of surfactant. The results showed that when the mass ratio of nano-TiO₂ and surfactant was about 1:2, the catalytic degradation effect of the material was the best.

Ma et al. applied TiO₂ nanoparticles to asphalt pavements to conduct an experimental investigation to purify vehicle emissions of asphalt and asphalt mixtures modified by nano-TiO₂ [19]. The results revealed that the TiO₂ nanoparticle was beneficial to increase the viscosity and reduced the temperature sensitivity which would enhance its high-

temperature stabilization capability of asphalt. It was also found that the incorporation of nano-TiO₂ in mixtures significantly enhance the rheometric properties of asphalt, the high temperature anti-rutting capacity and the anti-cracking properties, as well as water stabilization. Moreover, it verified that the nano-TiO₂-modified asphalt mixture possesses a positive impact on photocatalytic degradation of CH and NO_x.

3. Understanding Generation and Reduction Mechanism of Pollutant

3.1. Converting Nitrogen Oxide to Particulate Matter

Fine particulate matter (PM_{2.5}) is mainly formed by secondary organic aerosols (SOA) and secondary inorganic aerosols (SIA), which are generated from physical and chemical reactions between sulfur oxide (SO_x), nitrogen oxide (NO_x), volatile organic compounds (VOCs), ammonia (NH₃), and ozone (O₃) [20,21]. However, a detailed formation process and transformation mechanism of SOA has yet to be established, especially one that takes into account external factors such as nitrogen emissions from natural soils (biogenic soil nitrogen emission), regional ozone generation, nitrogen monoxide and nitrous oxide emission from natural forests, and temperature and climate conditions [22,23].

SOAs are formed through three main processes [24]. First, semi-volatile gas-phase products generated from reactions between atmospheric oxides (hydroxyl radical (OH), nitrate radical (NO₃), and ozone) move into the particulate phase through gas-particle partitioning. Second, large oligomer particles with molecular weights ranging from 100 to 1000 form through acid catalyzation on the surface of existing aerosols. Third, water-soluble organic compounds (WSOCs) in the atmosphere dissolve into cloud/mist droplets or fine particulate matter containing moisture and then move into the particulate phase (aqueous chemistry including OH reactions, and acid catalyzation).

SIAs are generated by chemical reactions of gas-phase precursors such as NO_x, SO₂, and NH₃ [21,24,25]. Ammonium nitrate (NH₄NO₃) and ammonium sulfate ((NH₄)₂SO₄) are the typical SIAs in the atmosphere, and ammonium nitrate is mainly generated by NO_x emissions from mobile pollution sources dominant on roads during the daytime [23,26]. Generation of NH₄NO₃ during the daytime begins with NO_x oxidation [27]. Nitrogen monoxide, emitted from NO_x emission sources such as mobile pollution, combines with ozone in the atmosphere to form nitrogen dioxide and reacts with hydroxyl radicals in the atmosphere to form nitric acid (HNO₃). Then, the nitric acid combines with ammonia to form ammonium nitrate.

3.2. Photocatalysis

The utilization of TiO₂ on pavement and road facilities has a significant effect on reducing NO concentration, a primary source of fine particulate matter. TiO₂ has a valence and conduction band, and the energy difference between the two bands (band gap energy). The band gap energy of TiO₂ in its anatase phase, which is mainly used as a photocatalyst, is 3.2 eV. When TiO₂ is applied on pavement and road facilities, the exposure to ultraviolet ray (UV) light greater than the band gap energy results in the formation of electrons (e⁻) and holes (h⁺). Those electrons and holes react with oxygen (O₂) and water (H₂O) in the air to generate active oxygen (superoxide anion (O₂⁻)) and hydroxyl radical (OH[·]) on the TiO₂ surface. Those products break down NO_x into nitrates (NO₃⁻), reducing NO_x in the atmosphere when they wash out as aqueous nitric acid (HNO₃[·]) solution in the rain. Moreover, nitrates (NO₃) can be removed through biological denitrification in groundwater [28]. The formulas for photocatalytic activity by ultraviolet rays described above are as follows [29]:



The process of removing the superoxide anion ($O_2^{\cdot-}$) and hydroxyl radical ($OH\cdot$) generated from reactions with NO_x are as follows:



The hydroxyl radical ($OH\cdot$) generated from the photocatalytic reaction in Equation (3) then reacts with NO and NO_2 according to Equations (5) and (6) to finally form nitric acid ($HNO_3\cdot$). Nitric acid ($HNO_3\cdot$) is water-soluble, so it can be easily removed from the photocatalytic surface by ambient air environments such as rain. Superoxide anion ($O_2^{\cdot-}$) generates water ($H_2O\cdot$), which in turn reacts with NO as detailed in Equation (7) to finally produce $HNO_3\cdot$ as shown in Equation (8). Also, NO molecules react with superoxide anion ($O_2^{\cdot-}$) to produce nitrates (NO_3^-), which is effective in removing NO_x [30].

4. Methodology

4.1. Characteristics of TiO_2 Material

Photocatalysts are substances that use light as an energy source to conduct catalytic reaction and applied in various areas for antibacterial, deodorizing and degradation of harmful substances. There are various types of photocatalysts including titanium dioxide (TiO_2), zinc oxide (ZnO), cadmium sulfide (CdS) and tungsten trioxide (WO_3) etc. ZnO and CdS generate harmful Zn and Cd ions by causing the catalyst itself to decompose by light. WO_3 has the disadvantage of having partial efficiency for specific substances. Since TiO_2 is stable chemically and physically and is not eroded by acids, bases, or organic solvents, it is widely used as a construction material [28]. Therefore, TiO_2 with anatase crystals was selected as photocatalyst for NO_x reduction for urban roads in this study. Figure 1 show a transmission electron microscopy image and the energy dispersive spectroscopy for TiO_2 material.

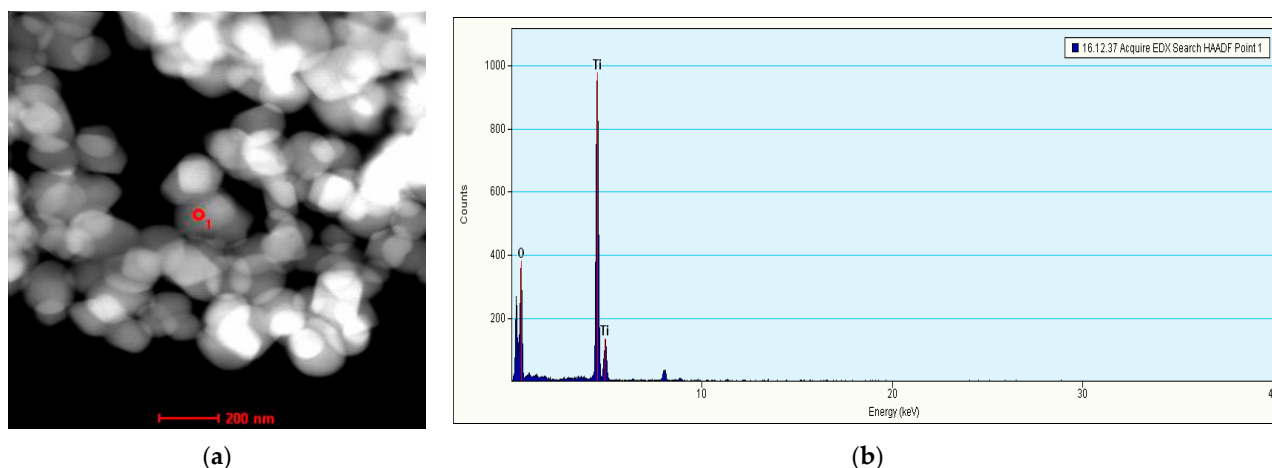


Figure 1. (a) Transmission electron microscopy image of TiO_2 ; (b) Energy dispersive spectroscopy image of TiO_2 .

4.2. Site Descriptions and Measurement Methods

On-site measurement of NO_x concentrations on urban roads is difficult due to the dispersion phenomena caused by winds or other weather conditions [31]. Wind speed and direction along with temperature and relative humidity have a significant role in the atmospheric dispersion of air pollutants [32]. In order to overcome the measurement limitations on urban roads, a 400 m-long underpass section located in Daegu, Korea was

selected as a field monitoring testbed for evaluating the NO_x reduction efficiency of a TiO₂ material applied on urban roads. The side walls in the underpass section enabled us to minimize the transportation of air pollutant in the horizontal direction.

The testbed was divided into two sections, a test section with TiO₂ applied and a reference section without TiO₂ applied. The average annual daily traffic at this testbed is approximately 13,000 vehicles. Since the test and reference section is located in a row at about 70 m distance, the effect of traffic characteristics on the NO_x concentration measured in the both sections are the same. A liquid type of TiO₂ was applied to the surface of asphalt pavement in the test section. A customized distributor vehicle with nozzles was used in uniform coverage of TiO₂ on the surface of asphalt pavement. The vehicle speed was calculated to spray the target amount of TiO₂. With 5 km/h of vehicle speed and 3 bar of injection pressure, 0.15 kg/m² of TiO₂ solution was applied uniformly on asphalt pavement. The data measured in the reference section reflects on the general characteristics of NO_x concentration in this testbed and will be used to estimate the NO_x reduction efficiency in the test section.

Data on NO_x concentration levels were measured at the test and reference section simultaneously to compare the trend of NO_x concentration in both sections and to reflect the characteristics of time series data for estimating probability distributions. In order to consider the effect of vehicle emission directly on NO_x concentration levels, the test probe was located 400 mm from the pavement surface. NO_x concentrations, traffic volume, and meteorological information were monitored from 16 to 20 December 2019 and from 3 to 7 February 2020. The NO_x concentration was measured using the chemiluminescence method, which is the set measurement standard based on the 'Framework Act on Environmental Policy' in Korea. In the chemiluminescence method, when nitrogen dioxide is produced by the reaction between nitrogen monoxide and ozone in the sample during the measurement of NO_x concentration, light is generated by transitional chemiluminescence to the activated molecular ground state. This method is a way to use the degree of light generated by those chemical lightings to be calculated in proportion to the concentration of nitric oxide.

Based on the meteorological information monitored at this testbed, the average temperature ranged from −2.1 to 9.1 °C and the average amount of cloud cover ranged from 0.8 to 6.0 Okta (in meteorology, an Okta is a unit of measurement used to describe the amount of cloud cover at any given location.). Also, the average wind speed ranged from 0.9 to 4.5 m/s and wind directions were mostly northwesterly during the measurement days. Tables 1 and 2 present the characteristics of on-site data collection and weather information during the measurement days, respectively.

4.3. Anderson-Darling Test

NO_x concentrations are generally calculated by applying a daily or time means to a reference concentration. However, the purpose of this study is to analyze the effect of TiO₂ on reducing NO_x concentration, and there is a limit to analyzing NO_x concentration changes since the NO_x analysis section will not reflect changes in NO_x concentration during a specific time or day. Therefore, in order to analyze the effect of TiO₂ on NO_x concentration reduction in this study, NO_x concentration was measured at a test section with TiO₂ applied and a reference section without TiO₂ applied. The data can then be analyzed by comparing how much of the NO_x analysis section is included in the range of 'high', defined as no less than 0.10 ppm, 'moderate', defined as no more than 0.10 ppm, and 'low', defined as no more than 0.06 ppm. In order to utilize this analysis method, first of all, the NO_x concentration in the test and reference section will be measured based on the unit time of 1 min over a certain time period. Then, probability distributions of each measured data set will be estimated using statistical inference methods. With each estimated probability distribution, the probability of NO_x occurring within the NO_x analysis ranges (high, moderate, low), which were defined in this study, can be analyzed by calculating the probability density function of each probability distribution.

Table 1. Characteristics of Data Collection.

Items	Contents
Location	Seopyung Underpass Section in Daegu, Korea
Characteristics of Testbed	Road Classification: Underpass Number of Lanes: 4 Lanes AADT: Approximately 13,000 Length of Testbed: Approximately 400 m
Description of Testbed	A General View of Testbed 
	Test Section with TiO ₂ applied 
	Reference Section without TiO ₂ applied 
Data Collection Devices	NO _x Measurement Device (Serinus 40 Oxides of Nitrogen Analyser) 
Date of Data Collection	16 to 20 December 2019 3 to 7 February 2020

Table 2. Weather Information of Measurement Days.

Date	Average Temperature (°C)	Average Cloud Cover (Okta)	Average Wind Speed (m/sec)	Wind Direction
16 December 2019	6.3	3.9	0.9	SE
17 December 2019	9.1	5.9	1.7	W
18 December 2019	7.4	5.3	3.1	NW
19 December 2019	4.1	4.3	4.1	NW
20 December 2019	2.4	6.0	2.0	NW
3 February 2020	3.6	2.0	2.9	NW
4 February 2020	1.9	0.8	1.8	W
5 February 2020	−1.5	1.1	4.5	NW
6 February 2020	−2.1	3.0	1.8	NW
7 February 2020	1.1	5.1	2.2	NW

First of all, to estimate the probability distribution of NO_x in the test and reference sections within the NO_x analysis ranges prescribed in this study, a goodness-of-fit test method can be used to determine how close the assumed probability distribution is to the empirical frequency distribution based on data obtained from the NO_x concentration measured from the test and reference sections [33,34]. Therefore, this study can use the Anderson-Darling test, which tests whether a set of data follows a specific distribution, as a goodness-of-fit verification method to determine the probability distribution suitable for the NO_x concentration data collected from the test and reference sections. The Anderson-Darling test is a statistical goodness-of-fit method presented by Anderson and Darling (1952) as a criterion for minimizing errors in the estimation process. This goodness-of-fit verification method is a method for verifying how much the data collected correspond to a characteristic distribution. The basic formula for the Anderson-Darling test is as follows [32]:

$$Q_n = n \int_{-\infty}^{\infty} [F_n(x) - F(x)]^2 \omega(x) dF(x) \quad (10)$$

where $F_n(x)$ is the empirical cumulative distribution function, $F(x)$ is the distribution function selected for analysis; and $\omega(x)$ is the weighting function.

In the basic formula, when $\omega(x) = [F(x)(1 - F(x))]^{-1}$, this is called the AD statistic and is commonly denoted as given by [31,32]:

$$A_n^2 = n \int_{-\infty}^{\infty} \frac{[F_n(x) - F(x)]^2}{F(x)(1 - F(x))} dF(x) \quad (11)$$

Also, some papers, including this study, give the following as the definition of the Anderson-Darling test statistic:

$$A_n^2 \approx - \sum (2i - 1) \left[\log(F(x_{(i)})) + \log(1 - F(x_{(n+1-i)})) \right]^{-n} \quad (12)$$

In the Anderson-Darling test, the higher the goodness-of-fit between the data and specific distributions, the smaller the AD statistics calculated are. In addition, p -value is used to determine which of the different distributions the data fits. If the p -value is less than the chosen significance level of 0.05, it is common to evaluate the goodness-of-fit between the data and a particular distribution as insignificant [32]. If the amount of data collected is large, the central limit theorem can be utilized rather than the data approximate the normal distribution. Therefore, if the amount of data measured is sufficient, normality verification is not required. However, if the data sample is smaller than 30, a normality

test should be implemented to find out the distribution. If it is not a normal distribution, a nonparametric method should be applied instead of a parametric method.

5. Analysis of the Effect of Titanium Dioxide on Reducing Nitrogen Oxide

5.1. Modeling of Nitrogen Oxide Reduction for Test and Reference Sections

The on-site data collected at the testbed was utilized to estimate the effect of TiO₂ on reducing NO_x concentration by stochastically analyzing and comparing the NO_x concentration in the test and reference section after eliminating abnormalities (outliers) during data collection. Next, the probability distribution of the NO_x concentration data measured at the test section and the reference section was estimated. The data collected can be analyzed based on a method of estimating the probability distribution using the probable goodness-of-fit between the measured data and a specific probability distribution. Thus, in this study, the probability of NO_x concentration measured at each section was estimated using the Anderson-Darling (AD) test among the different various goodness-of-fit verification methods. In the AD test, commonly used probability distributions include normal distribution, exponential distribution, Weibull distribution, and log-normal distribution. The probability distributions appropriate for the data collected from the test and reference section can be estimated based on AD statistics and *p*-value.

According to the results of the goodness-of-fit test for the probability distribution with the Anderson-Darling test, the AD statistics for the NO concentration distributions in the test section on 16 and 17 December 2019 were 1.631 (*p*-value: <0.010) and 7.296 (*p*-value: <0.010), respectively, with both following the Weibull distribution. The AD statistics for the NO_x concentration distributions in the reference section on the same dates were 2.341 (*p*-value: <0.010) and 9.501 (*p*-value: <0.010), respectively, with both following the Weibull distribution.

In addition, AD statistics for the NO_x concentration distributions in the test section on 18 December 2019 and 7 February 2020 were 1.315 (*p*-value: <0.005) and 2.868 (*p*-value: <0.005), which follow the log-normal distribution. Also, the AD statistics for the NO_x concentration distributions in the reference section on same dates as the test section were 0.551 (*p*-value: <0.005) and 0.869 (*p*-value: <0.010), which follow the log-normal distribution. For more detailed information on the results of the AD test, refer to Table 3 below.

Table 3. Results of Anderson-Darling Test in the Test and Reference Section.

Date		16 December 2019		17 December 2019		18 December 2019		19 December 2019		20 December 2019	
Types of Section		Test	Reference	Test	Reference	Test	Reference	Test	Reference	Test	Reference
AD Statistics	Normal	2.878	3.180	10.862	12.259	25.545	21.550	31.903	103.551	36.532	26.238
	Expon	61.302	67.425	31.854	46.012	47.735	75.952	50.181	55.544	13.269	30.366
	Weibull	1.631	2.341	7.296	9.501	9.938	12.408	14.719	36.982	10.941	9.586
	Log-Nor	5.339	4.451	10.367	11.979	1.315	0.551	3.660	2.305	4.448	3.559
<i>p</i> -value		<0.010	<0.010	<0.010	<0.010	<0.005	<0.005	<0.005	<0.005	<0.005	<0.005
Date		3 February 2020		4 February 2020		5 February 2020		6 February 2020		7 February 2020	
Types of Section		Test	Reference	Test	Reference	Test	Reference	Test	Reference	Test	Reference
AD Statistics	Normal	22.981	20.309	47.827	64.752	34.226	26.714	18.662	92.621	22.921	15.767
	Expon	28.169	49.699	18.046	24.871	47.036	61.648	67.007	85.200	29.684	55.967
	Weibull	7.921	10.634	123.97	17.898	11.544	11.191	7.906	41.041	7.965	6.796
	Log-Nor	0.951	1.264	3.992	2.458	0.242	0.630	0.595	1.328	2.868	0.869
<i>p</i> -value		<0.010	<0.005	<0.005	<0.005	<0.010	<0.010	<0.010	<0.005	<0.005	<0.010

Bold characters are the AD statistics of accepted distributions; Types of Section: Test→A segment of road with TiO₂ applied, Reference→A segment of road without TiO₂ applied.

The probability density function of each estimated probability distribution was computed to analyze the reduction effect of TiO₂ on NO_x concentration. This was calculated using the Anderson-Darling test with the probability distributions of each day measured and the two types of sections. The probability density function can be analyzed by comparing how much of the NO_x concentration is included in the range of above 0.10 ppm for

‘high’, between 0.06 and 0.10 ppm for ‘moderate’, and below 0.06 ppm for ‘low’. Figure 2 shows computational results of probability density function of each estimated distribution.

5.2. Evaluation of TiO₂ Effect on NO_x Reduction

Figure 3 shows a comparison of the daily mean NO_x concentration data measured in the test and reference sections. This figure reveals that NO_x concentration in the test section is generally lower than that in the reference section, indicating that use of TiO₂ is capable of reducing NO_x concentrations on urban roads. Table 4 presents the summary of analysis results for the NO_x concentration reduction effect with the descriptive statistics of measured data. On 16 December 2019, means of the NO_x concentration in the test and reference section were 0.213 ppm and 0.226 ppm, and the NO_x concentrations in each section were recorded to be between 0.043~0.504 ppm and 0.037~1.059 ppm, respectively. Also, from 17 to 20 December 2019 and 3 to 7 February 2020, means of NO_x concentration in the test section ranged from 0.047 to 0.218 ppm and in the reference section, it ranged from 0.077 to 0.219 ppm. During the same time period mentioned above, the NO_x concentrations are in the range between 0.002 to 0.789 ppm in the test section and 0.031 to 3.599 ppm in the reference section.

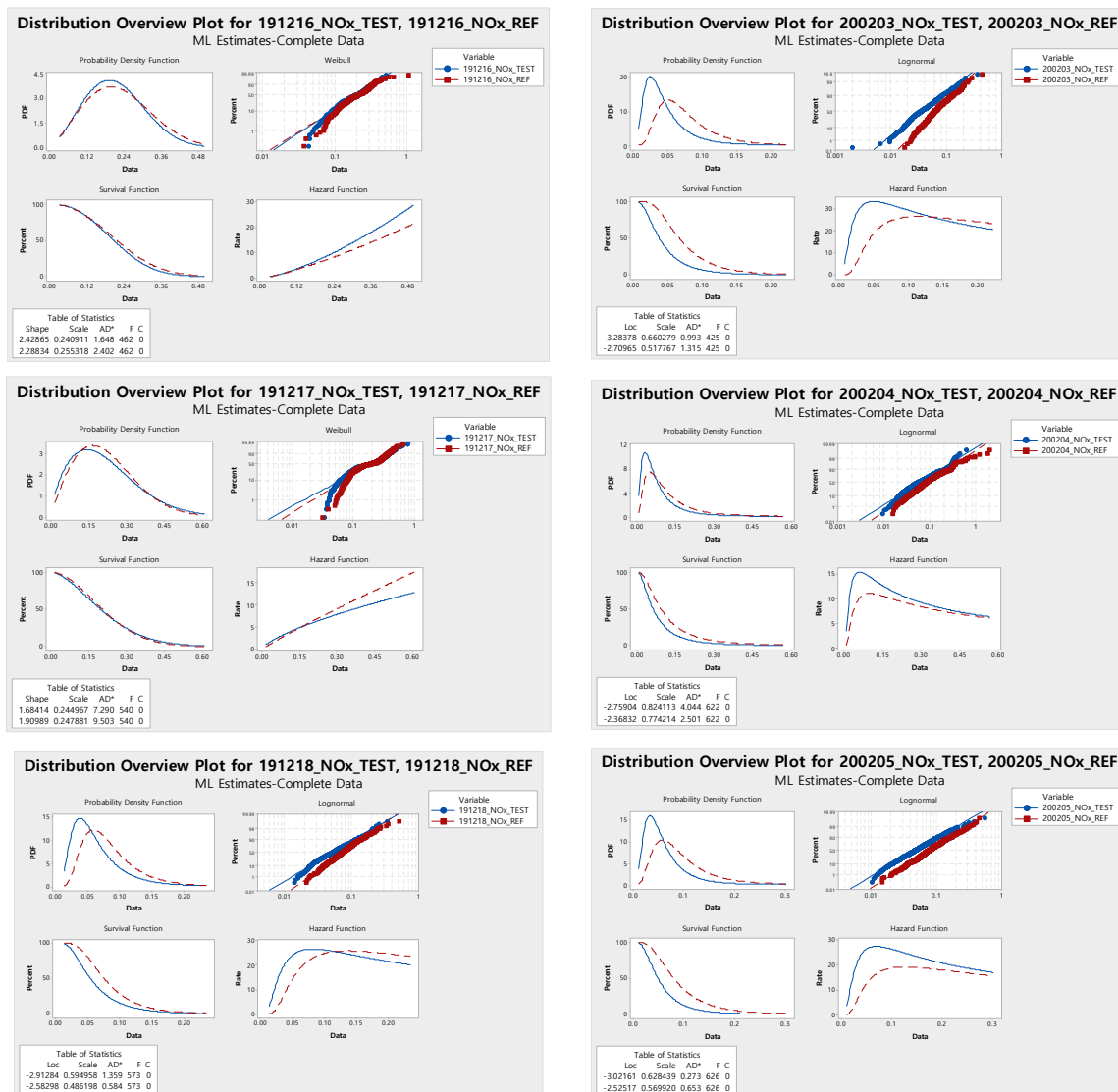


Figure 2. Cont.

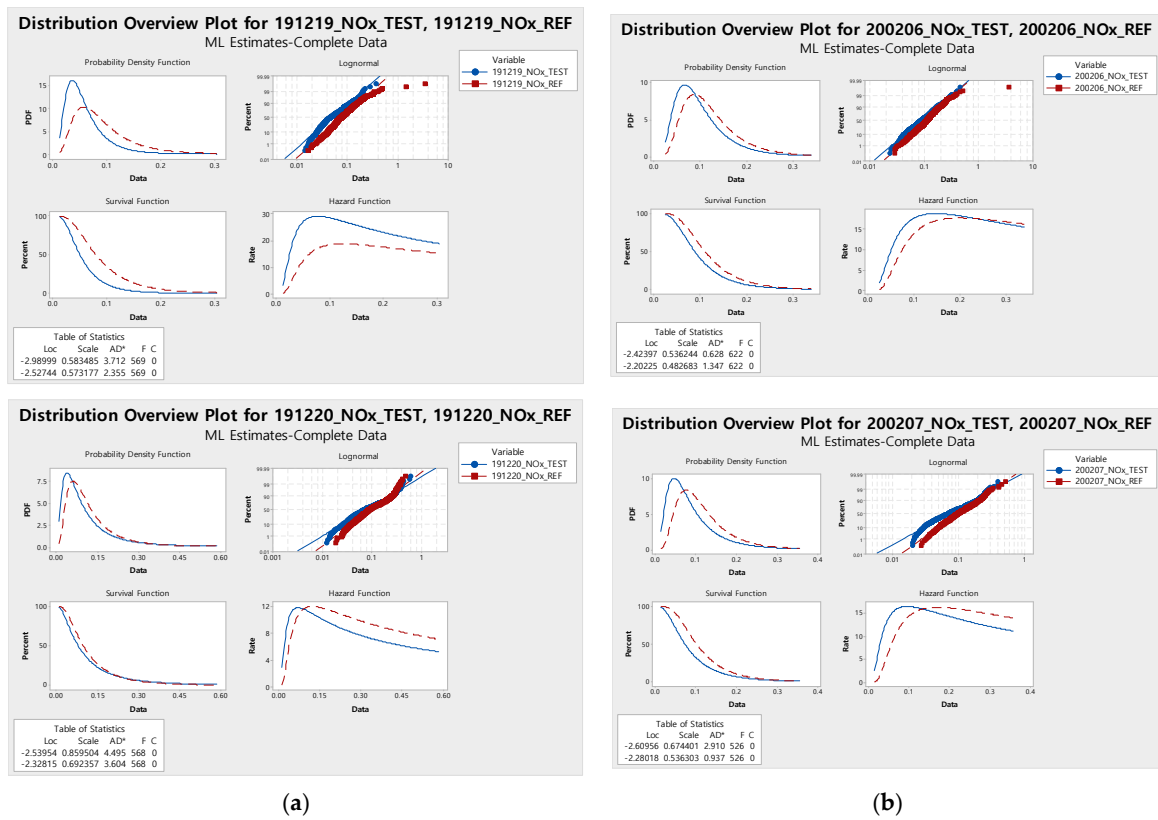


Figure 2. Probability distributions and probability density functions of the Anderson-Darling test for the test and reference sections: (a) Date of measurement: 6 to 20 December 2019; (b) Date of measurement: 3 to 7 February 2020.

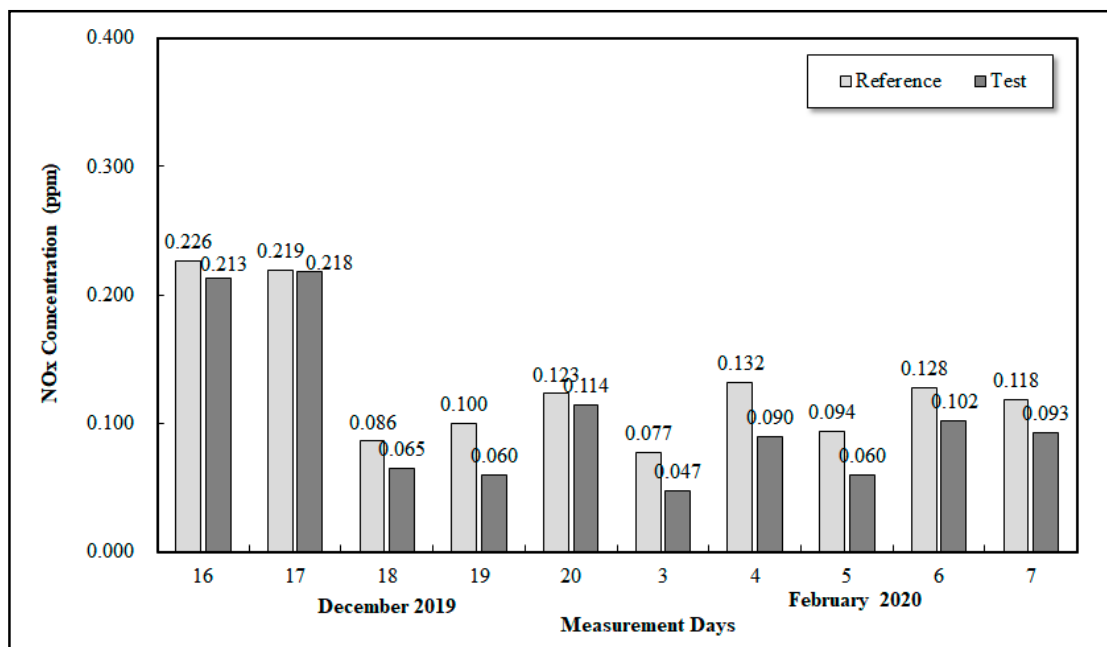


Figure 3. Means of NOx concentration on the test and reference section in measurement days.

Table 4. Analysis Results of Characteristics of NOx in the Test and Reference Section.

Date	Type of Sections	Number of Data	Mean (ppm)	Standard Deviation (ppm)	Max (ppm)	Min (ppm)	Distribution	Area from Probability Density Function (Probability of Inclusion in Standard Section)		
								High (>0.01 ppm)	Moderate (0.06~0.10 ppm)	Low (<0.06 ppm)
16 December 2019	Test	426	0.213	0.095	0.504	0.043	Weibull	88.9%	7.8%	3.3%
	Reference	426	0.226	0.103	1.059	0.037	Weibull	89.0%	7.4%	3.6%
17 December 2019	Test	540	0.218	0.135	0.789	0.033	Log-normal	80.2%	10.9%	8.9%
	Reference	540	0.219	0.122	0.656	0.031	Log-normal	83.8%	9.7%	6.5%
18 December 2019	Test	573	0.065	0.044	0.337	0.014	Log-normal	15.3%	28.1%	56.6%
	Reference	573	0.086	0.049	0.518	0.021	Log-normal	28.2%	40.0%	31.8%
19 December 2019	Test	569	0.060	0.042	0.378	0.015	Log-normal	11.9%	26.2%	61.9%
	Reference	569	0.100	0.164	3.466	0.017	Log-normal	34.7%	34.4%	30.9%
20 December 2019	Test	568	0.114	0.102	0.592	0.012	Log-normal	39.1%	23.4%	37.5%
	Reference	568	0.123	0.087	0.484	0.019	Log-normal	48.5%	27.3%	24.2%
3 February 2020	Test	425	0.047	0.037	0.361	0.002	Log-normal	6.9%	16.9%	76.2%
	Reference	425	0.077	0.047	0.437	0.018	Log-normal	21.6%	36.4%	42.0%
4 February 2020	Test	622	0.090	0.085	0.611	0.009	Log-normal	29.0%	23.6%	47.4%
	Reference	622	0.132	0.160	2.010	0.016	Log-normal	46.6%	25.1%	28.3%
5 February 2020	Test	626	0.060	0.047	0.550	0.010	Log-normal	12.6%	24.4%	63.0%
	Reference	626	0.094	0.061	0.452	0.015	Log-normal	34.8%	34.5%	30.7%
6 February 2020	Test	622	0.102	0.060	0.456	0.023	Log-normal	41.0%	35.6%	23.4%
	Reference	622	0.128	0.152	3.599	0.028	Log-normal	58.2%	31.5%	10.3%
7 February 2020	Test	526	0.093	0.066	0.400	0.020	Log-normal	32.4%	29.4%	38.2%
	Reference	526	0.118	0.068	0.522	0.028	Log-normal	51.7%	32.3%	16.0%

Types of Section: Test→A segment of the road with TiO₂ applied, Reference→A segment of the road without TiO₂ applied.

The NO_x concentrations in the testbed appeared in a rather wide range due to various factors such as atmospheric environment, weather conditions, and traffic characteristics during the measurement data. Moreover, the overall high level of NO_x concentration in this study can be attributed to the measurement of NO_x concentration at a close distance from passing vehicles.

Based on the analysis of the NO_x concentration reduction effect of TiO₂ using probability density functions, the occurrence probability of NO_x concentration in the test section on 18 December 2019 was 'high' at 15.3%, 'moderate' at 28.1%, and 'low' at 56.6%. The occurrence probability of NO_x concentration in the reference section on the same day was 'high' at 28.2%, 'moderate' at 40.0%, and 'low' at 31.8%. On 19 December 2019, the occurrence probability of NO_x concentration in the test section was 'high' at 11.9%, 'moderate' at 26.2%, and 'low' at 61.9%. In the reference section for the same date, the occurrence probability was 'high' at 34.7%, 'moderate' at 34.4%, and 'low' at 30.9%. Also, the occurrence probability of NO_x concentration in the test section on December 20th was 'high' at 39.1%, 'moderate' at 23.4%, and 'low' at 37.5%, while the occurrence probability of NO_x concentration in the reference section was 'high' at 48.5%, 'moderate' at 27.3%, and 'low' at 24.2%. In addition, the occurrence probability of NO_x concentration from 3 to 7 February 2020 follow a similar trend to the results from 18 to 20 December 2019.

However, the results of analysis on 16 and 17 December 2019 showed that the occurrence probability of NO_x concentration in the test section was 88.9% and 80.2% in 'high', 7.8% and 10.9% in 'moderate', 3.3% and 8.9% in 'low', respectively. The occurrence probability of NO_x concentration in the reference section on the two dates was analyzed as 89.0% and 83.8% in 'high', 7.4% and 9.7% in 'moderate', 3.6% and 6.5% in 'low'. This shows a slightly different result compared to other dates of measurement and could have been due to the effects of very cloudy weather conditions on the measurement of NO_x.

Comparing the occurrence probability of NO_x concentration between the test and reference sections, the average occurrence probability of NO_x concentration in the reference section in the 'high' range was about 28.1% higher than that of the test section, and in the case of 'moderate,' the average occurrence probability of the NO_x concentration in the reference section was about 18.8% higher than that of the test section. On the other hand, in the case of the 'low' range, the average probability of NO_x concentration in the test section was about 46.2% higher than that of the reference section. This fact indicated that the NO_x concentration in the test section was statistically lower comparing to the reference section.

It is well known that it is difficult to validate the reduction effect of TiO₂ using field experiments due to a large number of influencing variables such as wind speed, vehicle type, humidity, and temperature. However, it can be concluded from on-site measurement and statistical analysis that applying TiO₂ on asphalt pavement surfaces is capable of reducing the NO_x concentration through the photocatalytic reaction with sufficient solar radiation.

6. Summary and Conclusions

In this study, in order to analyze the effect of TiO₂ on reducing NO_x concentration, a full-scale testbed was constructed at an underpass section. A liquid type of TiO₂ was sprayed onto the surface of asphalt pavement in the test section, whereas no TiO₂ was applied on the reference section for comparison purposes. NO_x concentration was measured and collected at a one-minute interval in the two sections at the same time for 10 days. The reduction effects on NO_x concentration were analyzed by calculating the occurrence probability of the NO_x concentration in the test and reference sections using the Anderson-Darling test, which is a statistical verification method for the collected data.

According to the analysis results, most of the NO_x concentration data measured in the test section were probabilistically lower than those in the reference section. As a result, the average occurrence probability of the NO_x concentration in the reference section at 'high' and 'moderate' was about 28.1% and 18.8% higher than that of the test section, respectively. In the 'low' range, the average probability of NO_x concentration in the test

section was about 46.2% higher than that of the reference section. These results showed that the photochemical reaction of TiO₂ material applied on asphalt pavement was effective due to good weather conditions on the days of measurement.

In this study, an analysis of the reduction effect on NO_x concentration from applying TiO₂ onto road facilities is expected to be used in future studies for removing pollutants and gas precursors on urban roads. The on-site application of TiO₂ material at various types of road sections is required to validate the NO_x reduction efficiency by considering various influencing parameters. In the future, it is necessary to conduct long-term monitoring of NO_x concentration changes to evaluate the degradation of durability and reduction performance of the TiO₂ material utilized on the testbed.

Author Contributions: Conceptualization, S.-H.L. and H.-M.P.; methodology, S.-H.L.; software, S.-H.L.; validation, H.-M.P. and S.-H.L.; formal analysis, S.-H.L.; investigation, J.-W.L. and M.-K.K.; resources, H.-M.P., J.-W.L. and M.-K.K.; writing—original draft preparation, S.-H.L. and J.-W.L.; writing—review and editing, H.-M.P.; visualization, S.-H.L.; supervision, H.-M.P.; project administration, H.-M.P.; funding acquisition, H.-M.P. All authors have read and agreed to the published version of the manuscript.

Funding: This research received no external funding.

Institutional Review Board Statement: Not applicable.

Informed Consent Statement: Not applicable.

Data Availability Statement: Data sharing not applicable.

Acknowledgments: The authors are grateful for the financial support for the research from the Korea Institute of Civil Engineering and Building Technology (KICT).

Conflicts of Interest: The authors declare that there is no conflict of interests regarding the publication of this article.

References

1. Aldabe, J.; Elustondo, D.; Santamaria, C.; Lasheras, E.; Pandolfi, M.; Alsatuey, A.; Querol, X.; Santamaria, J.M. Chemical characterization and source apportionment of PM_{2.5} and PM₁₀ at rural, urban and traffic sites in Navarra (North of Spain). *Atmos. Res.* **2011**, *102*, 191–205. [CrossRef]
2. Wang, L.; Wang, J.; Tan, X.; Fang, C. Analysis of NO_x pollution characteristics in the atmospheric environment in Changchun city. *Atmosphere* **2020**, *11*, 30. [CrossRef]
3. Lee, K.; Park, W. The removal properties of NO_x with the photocatalytic (TiO₂) and UV optical science reactions. *J. Korea Acad. Ind. Coop. Soc.* **2010**, *11*, 3578–3582. [CrossRef]
4. Hackney, J.D.; Linn, W.S.; Buckley, R.D. Experimental studies on human health effects of air pollutants. *Arch. Environ. Health* **1975**, *30*, 373–378. [CrossRef]
5. Spengler, P.D.; Ferris, B.G.; Dockery, D.W.; Speizer, F.E. Sulfur dioxide and nitrogen dioxide levels inside and outside homes and the implications on health effects research. *Environ. Sci. Technol.* **1979**, *13*, 1276–1280. [CrossRef]
6. Katsouyanni, K.; Touloumi, G.; Spix, C.; Schwartz, J.; Balducci, F.; Medina, S.; Anderson, H.R. Short term effects of ambient Sulphur dioxide and particulate matter on mortality in 12 European cities: Results from time series data from the APHEA project. *Br. Med. J.* **1997**, *314*, 1658–1663. [CrossRef]
7. World Health Organization (WHO). Effects of Air Pollution on Children's Health and Development: A Review of the Evidence. 2005. Available online: <https://apps.who.int/iris/handle/10665/107652> (accessed on 20 September 2019).
8. Adams, M. Air Quality in Europe. Status and Opportunities. European Environmental Agency. 2017. Available online: http://mfvm.dk/fileadmin/user_upload/MFVM/Miljoe/Luftvision/EEA_Air_pollution_Ren_luftvision_1June2017.pdf (accessed on 18 May 2018).
9. Srimuruganandam, B.; Nagendra, S.S. Source characterization of PM₁₀ and PM_{2.5} mass using a chemical mass balance model at urban roadside. *Sci. Total Environ.* **2012**, *433*, 8–19. [CrossRef] [PubMed]
10. Jandacka, D.; Durcanska, D. Differentiation of particulate matter sources based on the chemical composition of PM₁₀ in functional urban areas. *Atmosphere* **2019**, *10*, 583. [CrossRef]
11. Mills, A.; Le Hunte, S. An overview of semiconductor photocatalysis. *J. Photochem. Photobiol. A Chem.* **1997**, *108*, 1–35. [CrossRef]
12. Devahasdin, S.; Fan, C., Jr.; Li, K.; Chen, D.H. TiO₂ photocatalytic oxidation of nitric oxide: Transient behavior and reaction kinetics. *J. Photochem. Photobiol. A Chem.* **2003**, *156*, 161–170. [CrossRef]
13. Chen, S.; Cao, G. Study on the photocatalytic oxidation of NO₂-ions using TiO₂ beads as a photocatalyst. *Desalination* **2006**, *194*, 127–134. [CrossRef]

14. Lasek, J.; Yu, Y.H.; Wu, J.C. Removal of NO_x by photocatalytic processes. *J. Photochem. Photobiol. C Photochem. Rev.* **2013**, *14*, 29–52. [[CrossRef](#)]
15. Folli, A.; Strøm, M.; Madsen, T.P.; Henriksen, T.; Lang, J.; Emenius, J.; Klevebrant, T.; Nilsson, Å. Field study of air purifying paving elements containing TiO₂. *Atmos. Environ.* **2015**, *107*, 44–51. [[CrossRef](#)]
16. Bocci, E.; Riderelli, L.; Fava, G.; Bocci, M. Durability of NO oxidation effectiveness of pavement surfaces treated with photocatalytic titanium dioxide. *Arab. J. Sci. Eng.* **2016**, *41*, 4827–4833. [[CrossRef](#)]
17. Wang, D.; Leng, Z.; Yu, H.; Hüben, M.; Kollmann, J.; Oeser, M. Durability of epoxy-bonded TiO₂-modified aggregate as a photocatalytic coating layer for asphalt pavement under vehicle tire polishing. *Wear* **2017**, *382*, 1–7. [[CrossRef](#)]
18. Yu, H.; Dai, W.; Qian, G.; Gong, X.; Zhou, D.; Li, X.; Zhou, X. The NO_x degradation performance of Nano-TiO₂ coating for asphalt pavement. *Nanomaterials* **2020**, *10*, 897. [[CrossRef](#)] [[PubMed](#)]
19. Ma, Y.Z.; Li, L.L.; Wang, H.; Wang, W.S.; Zheng, K.K. Laboratory study on performance evaluation and automobile exhaust degradation of nano-TiO₂ particles-modified asphalt materials. *Adv. Mater. Sci. Eng.* **2021**, *2021*, 5574013. [[CrossRef](#)]
20. Zhang, Q.; Jimenez, J.L.; Canagaratna, M.R.; Ulbrich, I.M.; Ng, N.L.; Worsnop, D.R.; Sun, Y. Understanding atmospheric organic aerosols via factor analysis of aerosol mass spectrometry: A review. *Anal. Bioanal. Chem.* **2011**, *401*, 3045–3067. [[CrossRef](#)]
21. Huang, R.J.; Zhang, Y.; Bozzetti, C.; Ho, K.F.; Cao, J.J.; Han, Y.; Daellenbach, K.R.; Slowik, J.G.; Platt, S.M.; Canonaco, F. High secondary aerosol contribution to particulate pollution during haze events in china. *Nature* **2014**, *514*, 218–222. [[CrossRef](#)]
22. Li, K.; Chen, L.; Han, K.; Lv, B.; Bao, K.; Wu, X.; Gao, X.; Cen, K. Smog chamber study on aging of combustion soot in isoprene/SO₂/NO_x system: Changes of mass, size, effective density, morphology and mixing state. *Atmos. Res.* **2017**, *184*, 139–148. [[CrossRef](#)]
23. Kaltsonoudis, C.; Jorga, S.D.; Louvaris, E.; Florou, K.; Pandis, S.N. A portable dual-smog-chamber system for atmospheric aerosol field studies. *Atmos. Meas. Tech.* **2019**, *12*, 2733–2743. [[CrossRef](#)]
24. Lim, Y.B.; Lee, S.B.; Kim, H.; Kim, J.Y.; Bae, G.N. Review of recent smog chamber studies for secondary organic aerosol. *J. Korean Soc. Atmos. Environ.* **2016**, *32*, 131–157. [[CrossRef](#)]
25. Squizzato, S.; Masiol, M.; Brunelli, A.; Pistollato, S.; Tarabotti, E.; Rampazzo, G.; Pavoni, B. Factors determining the formation of secondary inorganic aerosol: A case study in the po valley (italy). *Atmos. Chem. Phys.* **2013**, *13*, 1927–1939. [[CrossRef](#)]
26. Ge, X.; He, Y.; Sun, Y.; Xu, J.; Wang, J.; Shen, Y.; Chen, M. Characteristics and formation mechanisms of fine particulate nitrate in typical urban areas in china. *Atmosphere* **2017**, *8*, 62. [[CrossRef](#)]
27. Nowak, J.B.; Neuman, J.A.; Bahreini, R.; Brock, C.A.; Middlebrook, A.M.; Wollny, A.G.; Holloway, J.S.; Peischl, J.; Ryerson, T.B.; Fehsenfeld, F.C. Airborne observations of ammonia and ammonium nitrate formation over Houston, Texas. *J. Geophys. Res. Atmos.* **2010**, *115*. [[CrossRef](#)]
28. Lee, J.W.; Jang, Y.I.; Park, W.S.; Kim, S.W.; Lee, B.J. Photocatalytic and pozzolanic properties of nano-SiO₂/Al₂O₃-TiO₂ powder for functional mortar. *Materials* **2019**, *12*, 1037. [[CrossRef](#)] [[PubMed](#)]
29. Dalton, J.S.; Janes, P.A.; Jones, N.G.; Nicholson, J.A.; Hallam, K.R.; Allen, G.C. Photocatalytic oxidation of NO_x gases using TiO₂: A surface spectroscopic approach. *Environ. Pollut.* **2002**, *120*, 415–422. [[CrossRef](#)]
30. Seo, J.H.; Yoon, H.N.; Kim, S.H.; Bae, S.J.; Jang, D.I.; Kil, T.K.; Park, S.M.; Lee, H.K. An overview on the physicochemical properties and photocatalytic pollutant removal performances of TiO₂-incorporated cementitious composites. *Compos. Res.* **2020**, *33*, 68–75. [[CrossRef](#)]
31. Saha, P.K.; Khlystov, A.; Snyder, M.G.; Grieshop, A.P. Characterization of air pollutant concentrations, fleet emission factors, and dispersion near a North Carolina interstate freeway across two seasons. *Atmos. Environ.* **2018**, *177*, 143–153. [[CrossRef](#)]
32. Gulia, S.; Nagendra, S.S.; Khare, M. A system based approach to develop hybrid model predicting extreme urban NO_x and PM_{2.5} concentration. *Transp. Res. Part D Transp. Environ.* **2017**, *56*, 141–154. [[CrossRef](#)]
33. Shin, H.J.; Sung, K.M.; Heo, J.H. Derivation of modified Anderson-Darling test statistics and power test for the Gumbel distribution. *J. Korea Water Resour. Assoc.* **2010**, *43*, 813–822. [[CrossRef](#)]
34. Lee, S.H.; Park, H.M. Analysis of characteristics of fine particulate matter concentrations using statistical methods. *Int. J. Highw. Eng.* **2019**, *21*, 121–132. [[CrossRef](#)]